Electronic supplementary information (ESI)

A Long-Lived Photo-Induced Metastable State of Linkage Isomerization Accompanied with a Spin Transition

Chou-Fu Sheu,[a] Che-Hsiu Shih,[b,c] Kunihisa Sugimoto,[c,d] Bing-Ming Cheng,[e] Masaki Takata,[b,c,d] Yu Wang*[a]

[a]Department of Chemistry, National Taiwan University, Taipei, 10617 Taiwan, R.O.C.; Tel: +886-2-33661654; E-mail: wangyu@ntu.edu.tw; [b]Department of Advanced Materials Science, University of Tokyo, Kashiwa, Chiba 277-8561, Japan.; [c]RIKEN SPring-8 center, Sayo, Hyogo 679-5148, Japan. [d]Japan Synchrotron Radiation Research Institute, Sayo, Hyogo 679-5148, Japan. [e]National Synchrotron Radiation Research Center, Hsinchu, 30076 Taiwan, R.O.C.

Table of Contents:

(1) Sample preparation:

There are four polymorphs of complex *trans*-Fe(abpt)$_2$(NCS)$_2$; to avoid the possible contamination of other polymorphs, polymorph D was prepared in single crystal forms by diffusion method which was described in the literature.[S1] Single crystals of polymorph D can be identified under microscope in its red color and needle shape morphology. Sample used for physical study was carefully isolated by hand under microscope.

(2) FTIR measurements and results:

The FTIR spectra were recorded using a Bomem DA8 FTIR spectrometer. The sample was prepared by grinding crystals together with KBr to fine powder, and then pressed into disk. For low temperature measurements, the disc was glued to a holder on the cold head of a close-cycle cryostat (APD), which can be operated in the temperature range 15-300 K.

For thiocyanate-coordinated SCO iron(II) complexes, the C≡N stretching frequency ($\nu_{C\equiv N}$) shifted significantly[S2,S3] associated with HS and LS states. Taking advantage of the strong signal of such stretching vibration in the range of 1900-2200 cm^{-1}, it is used to monitor the change in spin state at various conditions. At 300K, two peaks are found at 2050 and 2079 cm^{-1} shown in Figure S1, which correspond to the HS states of two crystallographically independent iron (Fe2 and Fe1) sites.[S1] The peak at 2079 cm^{-1}, becomes weaker and concurrently a new peak at 2120 cm^{-1} becomes stronger as the temperature goes below 175 K, the relative intensities of absorption bands at 2079 and 2120 cm^{-1} therefore correlate directly to the HS and LS configurations of Fe1 respectively. At 15 K, the metastable HS is successfully achieved in hundred percent by the irradiation of light at 532 nm, when the peak at 2120 cm^{-1} of LS state vanishes. Further warming of such metastable state to 65 K in dark, the relaxation to LS state occurs as indicated by the re-appearance of the peak at 2120 cm^{-1}. With the temperature higher than T_{LIESST} (=36 K, determined from photomagnetic experiment), the spectrum is expected to be exactly the same as the one at 65 K before the laser irradiation. However, the peaks at 2079 cm^{-1} does show complicated features, which suggest the existence of other metastable state during the light irradiation process. The metastable state was further confirmed by photomagnetic and photocrystallographic experiments.

(3) Magnetic measurements:

The magnetic susceptibilities were measured with a Quantum Design SQUID magnetometer MPMS-XL7. The photomagnetic experiment was achieved by using an

optical fiber to guide the laser light source into the SQUID magnetometer. For sample preparation, dozens of small single crystals were arranged under microscope to one single layer inside a quartz holder with small quantity of vacuum grease to ensure the light penetration, and then placed on the end of the optical fiber.

(4) X-ray crystallography:

Crystallographic experiments were conducted at beamline BL02B1 in SPring-8 synchrotron facility. A Rigaku large cylindrical image-plate with the size of 350 mm x 683 mm was used as the detector. An open-flow helium cryosystem was used to reach the required temperature, which was calibrated by the phase transition (tetragonal to orthorhombic) of single crystal $TbVO_4$ at Tc = 32 K. The excitation laser with wavelength 532 nm was chosen to avoid the maximum absorption of metal to ligand charge transfer band at 500 nm, the penetration depth of ~100 μm are estimated from the extinction coefficient.[S4] From the photomagnetic relaxation experiments at various temperature, the metastable **MS-1** species relax significantly even at 20 K (Figure S2). Therefore the photocrystallographic experiments were performed under continuous laser irradiation.

All the peak profiles were indexed and integrated using RAPID AUTO.[S5] For data set (1 & 2), the structures can be solved by direct method and refined on F^2 with full-matrix least squares. All non-hydrogen atoms were refined with anisotropic displacement parameters. The pyridyl hydrogen atom positions were fixed geometrically at calculated distances and allowed to ride on the parent carbon atoms. Details of the crystal data and refinement are given in Table S1 and S2.

Structure refinements of crystallographic data set (3)

According to FTIR and photomagnetic studies, only the Fe1 sites will be light-induced from LS to a major product of **MS-2** and a minor product of **MS-1** at 20 K. The structure refinement was then started by introducing a rigid-body molecular structure **MS-1**, which was obtained from the data set (2). The difference Fourier maps show large negative electron density at the positions of Fe1 and N3-C13-S1, which are in agreement with the existence of another major product (Figure S6 (a)). Three strongest residuals (50, 30 and 25 $eÅ^{-3}$) can be assigned to the Fe3, S3 and S4 positions of **MS-2** judged by their values and positions. The next step for structure refinement was to apply the rigid-body part only on the thiocyanate ligand of **MS-1,** and the distance of the nitrogen (N3) to Fe1 was fixed. The sum of site occupancy factor (SOF) for the iron and sulfur of **MS-1** and **MS-2** was confined to 1. The C27, C28 N15 and N16 atoms on the thiocyanate of **MS-2** can be located without difficulty from the difference Fourier maps by the four major residuals (> 6 $eÅ^{-3}$) and the linear feature (Figure S6 (b)). The Fe3

was found to shift away (~0.4 Å) from the crystallographic inversion center and two NCS were located, that indicated a non-centrosymmetric **MS-2** molecule equally disordered over two orientations related to the crystallographic inversion center in the crystal (Figure S6 (c)).

The ligand abpt was refined without disordered treatment. Therefore, the shorter Fe1 to N(abpt) distances in the final result indicate that the actual Fe-N(abpt) distances for **MS-2** are slightly shorter than that of **MS-1** (Table S5). Except the disorder parts on the iron and thiacyanate, all non-hydrogen atoms were refined with anisotropic displacement parameters.

A residual peak 4.2 eÅ^{-3}, located at 0.70 Å from the position of S1 atoms and 0.59 Å from N15 in the final difference maps (Q1 on Figure S6 (c)), may come from a disorder of N16-C28-S4 of **MS-2**. This kind of disorder is not rare on thiocyanate-containing metal complexes.[S6] The structure was further refined on the account of the disorder of N16-C28-S4, The R1 value decreases from 0.0519 to 0.043 with the largest positive/negative residual peak 1.5 / -0.6 eÅ^{-3} in the final difference maps. Details of the crystal data and refinement are given in Table S3.

Structure refinements of crystallographic data set (4)

For data set (4), the structure refinement procedure was exactly the same as that of data set (3), only the starting rigid-body part was molecular structure of **GS** from data set (1). The bond distances of Fe1-N(abpt) are shorter than those of the data set (3) (Table S5), which is consistent with the relaxation of **MS-1** to **GS** after temperature was raised to 65 K. Details of the crystal data and refinement are given in Table S4.

The N16-C28-S4 disorder with 0.80/0.20 population of two orientations was further applied on of **MS-2**, The R1 value decreases from 0.057 to 0.050 with the largest positive/negative residual peak 1.5 / -0.8 eÅ^{-3} in the final difference maps.

(5) Details of crystal data and structure refinement:

Table S1. Crystal data and structure refinement for **GS** state from data set(1)

Empirical formula	$C_{26}\ H_{20}\ N_{14}\ S_2\ Fe$
Formula weight	648.53
Temperature	20(2) K
Wavelength	0.49812 Å
Crystal system, space group	Monoclinic, $P2_1/c$
Unit cell dimensions	a = 10.7906(2) Å
	b = 15.6885(2) Å, beta = 107.5972(7)°
	c = 16.9891(7) Å
Volume	2741.47(13) $Å^3$
Z, Calculated density	4, 1.571 Mg/m^3
Absorption coefficient	0.285 mm^{-1}
F(000)	1328
Crystal size	0.10 x 0.07 x 0.07 mm
Theta range for data collection	1.67 to 24.53 deg.
Limiting indices	-17<=h<=17, -26<=k<=26, -28<=l<=28
Reflections collected / unique / observed	47941 / 13154 [R(int) = 0.0379] / 12100
Completeness of data	99 %
Absorption correction method	Multi-Scan
Refinement method	Full-matrix least-squares on F^2
Data / restraints / parameters	13154 / 0 / 407
Goodness-of-fit on F^2	1.051
Final R indices [I>2sigma(I)]	$R1$ = 0.0287, $wR2$ = 0.0790
R indices (all data)	$R1$ = 0.0313, $wR2$ = 0.0814
Largest diff. peak and hole	0.687 and -0.668 e.$Å^{-3}$

$R(\text{int}) = \Sigma|F_o^2 - F_o^2(\text{mean})| / \Sigma[F_o^2]$, $R1 = \Sigma||F_o| - |F_c|| / \Sigma|F_o|$, $wR2 = \{\Sigma[w(F_o^2 - F_c^2)^2] / \Sigma[w(F_o^2)^2]\}^{1/2}$, $\text{GooF} = S = \{\Sigma[w(F_o^2 - F_c^2)^2] / (n - p)\}^{1/2}$; n is the number of reflections and p is the total number of parameters refined.

Table S2. Crystal data and structure refinement for **MS-1** from data set (2), crystal was under continuous 532 nm laser irradiation with a power of 5 mW/cm^2

Empirical formula	$C_{26}\ H_{20}\ N_{14}\ S_2\ Fe$
Formula weight	648.53
Temperature	20 (2) K
Wavelength	0.49812 Å
Crystal system, space group	Monoclinic, $P2_1/c$
Unit cell dimensions	a = 10.7210(2) Å
	b = 15.8909(2) Å, beta = 106.0191 (7)º
	c = 17.1861(7) Å
Volume	2814.24(13) Å^3
Z, Calculated density	4, 1.531 Mg/m^3
Absorption coefficient	0.279 mm^{-1}
F(000)	1328
Crystal size	0.10 x 0.07 x 0.07 mm
Theta range for data collection	1.25 to 24.48 deg.
Limiting indices	-16<=h<=17, -26<=k<=26, -23<=l<=28
Reflections collected / unique / observed	31788 / 13095 [R(int) = 0.0355] / 11126
Completeness of data	96.5 %
Absorption correction method	Multi-Scan
Refinement method	Full-matrix least-squares on F^2
Data / restraints / parameters	13095 / 0 / 407
Goodness-of-fit on F^2	1.055
Final R indices [I>2sigma(I)]	$R1$ = 0.0334, $wR2$ = 0.0912
R indices (all data)	$R1$ = 0.0416, $wR2$ = 0.0944
Largest diff. peak and hole	0.777 and -0.536 e.Å^{-3}

$R(\text{int}) = \Sigma|F_o^2 - F_o^2(\text{mean})| / \Sigma[F_o^2]$, $R1 = \Sigma||F_o| - |F_c|| / \Sigma|F_o|$, $wR2 = \{\Sigma[w(F_o^2 - F_c^2)^2] / \Sigma[w(F_o^2)^2]\}^{1/2}$, GooF = S = $\{\Sigma[w(F_o^2 - F_c^2)^2] / (n - p)\}^{1/2}$; n is the number of reflections and p is the total number of parameters refined.

Table S3. Crystal data and structure refinement for **MS-2/MS-1** from data set (3), crystal under continuous irradiation continuous 532 nm laser irradiation with a power of 40 mW / cm^2

Empirical formula	$C_{26}\ H_{20}\ N_{14}\ S_2\ Fe$
Formula weight	648.53
Temperature	20 (2) K
Wavelength	0.4959 Å
Crystal system, space group	Monoclinic, $P2_1/c$
Unit cell dimensions	a = 10.6323(3) Å
	b = 15.8857(4) Å, beta = 105.9133 (7)º
	c = 17.2296(7) Å
Volume	2798.59(16) $Å^3$
Z, Calculated density	4, 1.539 Mg/m^3
Absorption coefficient	0.277 mm^{-1}
F(000)	1328
Crystal size	0.08 x 0.08 x 0.03 mm
Theta range for data collection	1.24 to 24.62 deg.
Limiting indices	-17<=h<=17, -26<=k<=25, -28<=l<=28
Reflections collected / unique / observed	40592 / 13701 [R(int) = 0.0422] / 11041
Completeness of data	98.5 %
Absorption correction method	Multi-Scan
Refinement method	Full-matrix least-squares on F^2
Data / restraints / parameters	13701 / 0 / 415
Goodness-of-fit on F^2	1.048
Final R indices [I>2sigma(I)]	$R1$ = 0.0432, $wR2$ = 0.1061
R indices (all data)	$R1$ = 0.0573, $wR2$ = 0.1133
Largest diff. peak and hole	1.498 and -0.607 e.$Å^{-3}$

$R(\text{int}) = \Sigma|F_o^2 - F_o^2(\text{mean})| / \Sigma[F_o^2]$, $R1 = \Sigma||F_o| - |F_c|| / \Sigma|F_o|$, $wR2 = \{\Sigma[w(F_o^2 - F_c^2)^2] / \Sigma[w(F_o^2)^2]\}^{1/2}$, $\text{GooF} = S = \{\Sigma[w(F_o^2 - F_c^2)^2] / (n - p)\}^{1/2}$; n is the number of reflections and p is the total number of parameters refined.

Table S4. Crystal data and structure refinement for **MS-2/GS** from data set (4), the temperature of the crystal is raised to 65 K for half an hour after data collection of data set (3)

Empirical formula	$C_{26}\ H_{20}\ N_{14}\ S_2\ Fe$
Formula weight	648.53
Temperature	20 (2) K
Wavelength	0.4959 Å
Crystal system, space group	Monoclinic, $P2_1/c$
Unit cell dimensions	a = 10.6715(6) Å
	b = 15.8611(2) Å, beta = 106.252 (4)º
	c = 17.1977(6) Å
Volume	2794.58(18) $Å^3$
Z, Calculated density	4, 1.541 Mg/m^3
Absorption coefficient	0.278 mm^{-1}
F(000)	1328
Crystal size	0.08 x 0.08 x 0.03 mm
Theta range for data collection	1.24 to 24.41 deg.
Limiting indices	-17<=h<=17, -26<=k<=25, -28<=l<=28
Reflections collected / unique / observed	42088 / 13411 [R(int) = 0.0611] / 11113
Completeness of data	99.0 %
Absorption correction method	Multi-Scan
Refinement method	Full-matrix least-squares on F^2
Data / restraints / parameters	13411 / 0 / 415
Goodness-of-fit on F^2	0.995
Final R indices [I>2sigma(I)]	$R1$ = 0.0499, $wR2$ = 0.1278
R indices (all data)	$R1$ = 0.0623, $wR2$ = 0.1345
Largest diff. peak and hole	1.490 and -0.754 $e.Å^{-3}$

$R(\text{int}) = \Sigma|F_o^2 - F_o^2(\text{mean})| / \Sigma[F_o^2]$, $R1 = \Sigma||F_o| - |F_c|| / \Sigma|F_o|$, $wR2 = \{\Sigma[w(F_o^2 - F_c^2)^2] / \Sigma[w(F_o^2)^2]\}^{1/2}$, $\text{GooF} = S = \{\Sigma[w(F_o^2 - F_c^2)^2] / (n - p)\}^{1/2}$; n is the number of reflections and p is the total number of parameters refined.

(6) Selected bond length and bond angle:

Table S5. Selected bond length and bond angle

data set	(1)	(2)	(3)	(4)
Spin state	LS	HS	HS	Mix
		Bond distance (Å)		
Fe1-$N1_{abpt}$	1.9956(6)	2.1844(7)	2.116(1)	2.089(1)
Fe1-$N2_{abpt}$	1.9825(6)	2.1536(7)	2.102(1)	2.076(1)
Fe1-$N3_{NCS}$	1.9485(7)	2.1359(9)	2.187(2)	1.962(2)
Fe3-$N16_{NCS}$			2.040(3)	2.020(2)
Fe3-$S3_{SCN}$			3.326(1)	3.344(1)
		Bond angle (°)		
Fe3-N16-C28			173.2(3)	174.5(3)
Fe3-S3-C27			140.3(1)	140.3(1)

The Fe3 is referring to the iron of **MS-2** (linkage isomer)

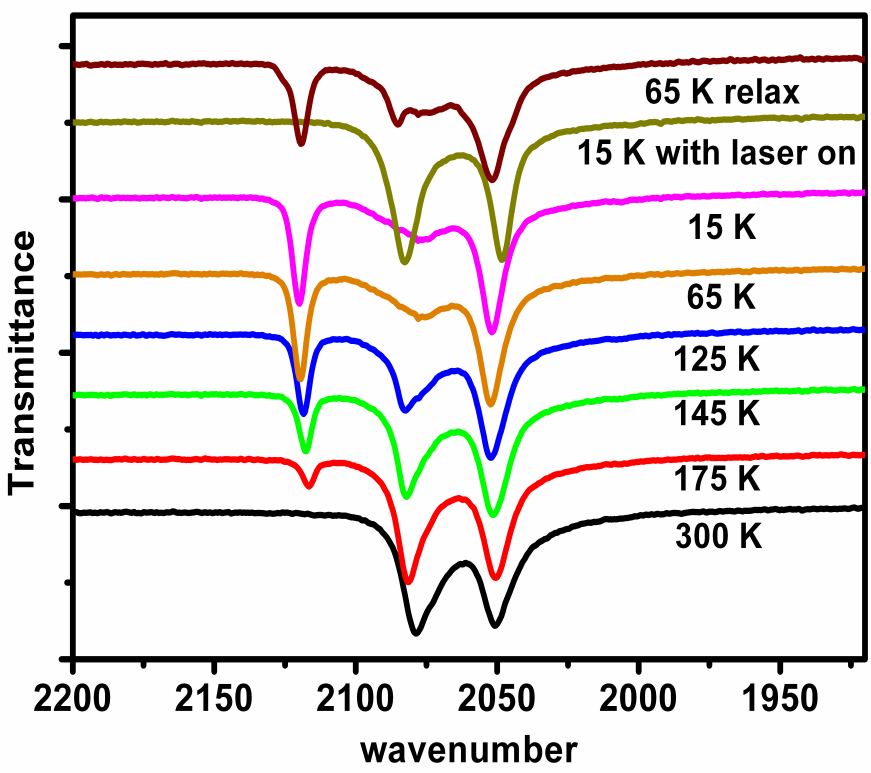

Figure S1. FTIR spectra in the range of CN stretching frequency at different temperatures, and after 532 nm laser light irradiation; 'relax' means to warm up to 65 K after the light is turned off.

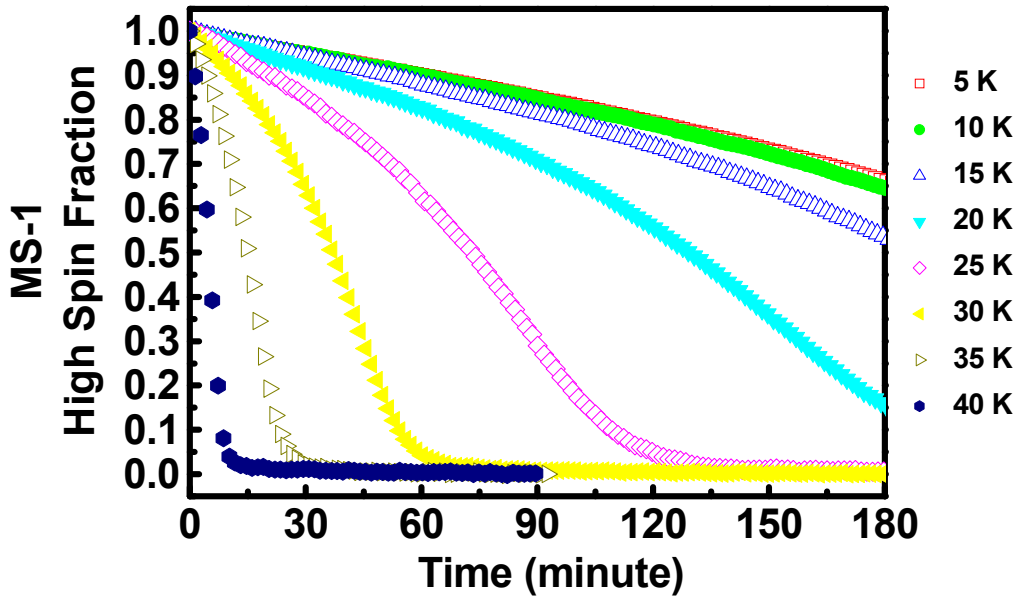

Figure S2. Temperature-dependent relaxation data of **MS-1** determined from photomagnetic measurements.

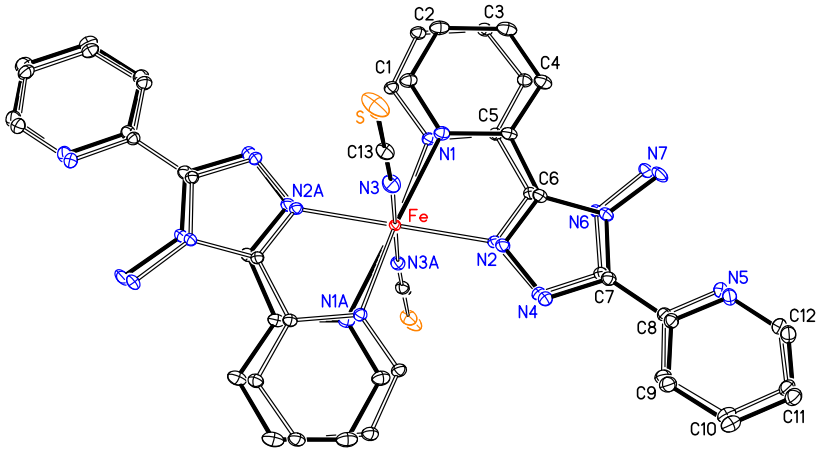

Figure S3. The superimposed molecular structures of **GS** (open bonds; data set (1)) and **MS-1** (solid bonds, data set (2)) at 20 K. Thermal ellipsoids are plotted at 50% probability.

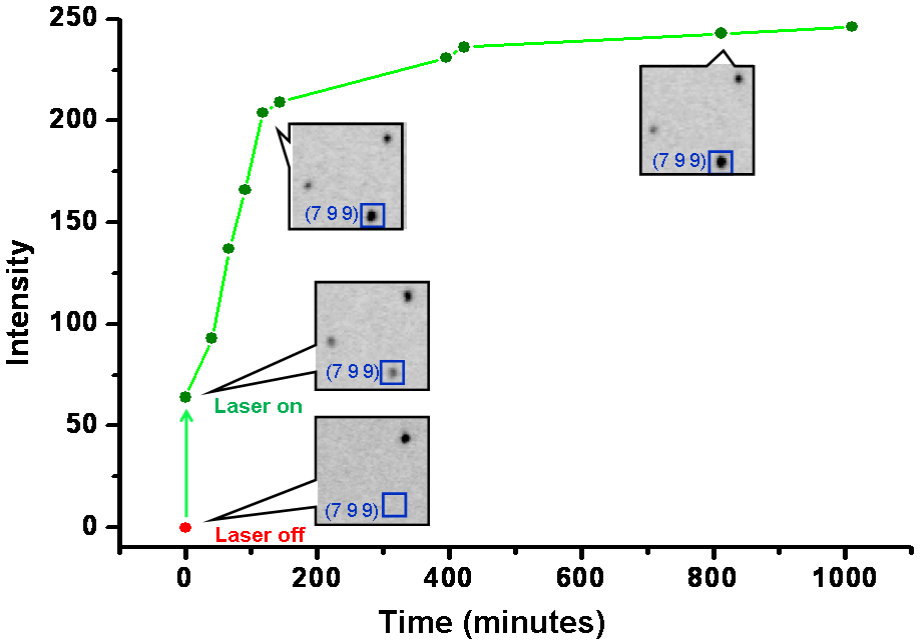

Figure S4. Time evolution of the diffraction peak (7 9 9), which is only proportional to the quantity of molecules at **MS-2**; the peak is unobserved at **GS** and **MS-1**, but is getting stronger with time during laser irradiation, which corresponds to the formation of **MS-2** state. It takes about 10 hours to reach this steady state.

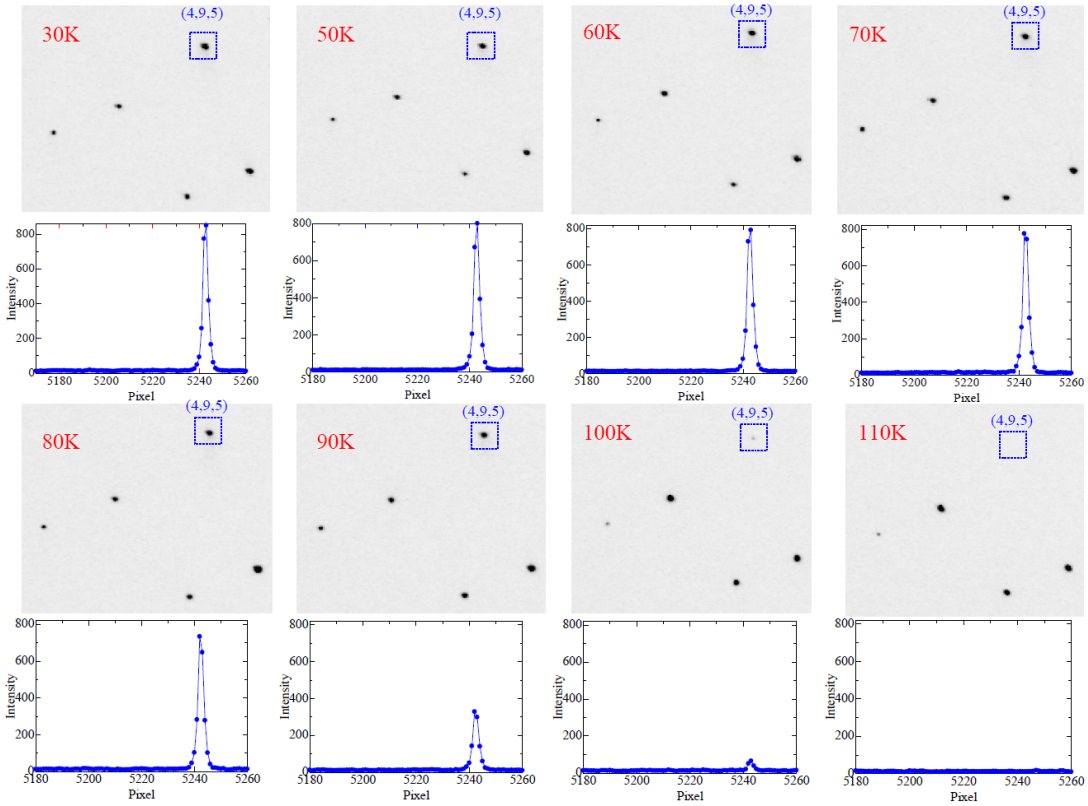

Figure S5. The intensity of reflection (4 9 5) is unobserved at **GS**, which is used to monitor the relaxation of **MS-2** as temperature raises. The intensity vanished at 110 K indicating the complete relaxation of thiocyanate S-coordinated to N-coordinated ground state.

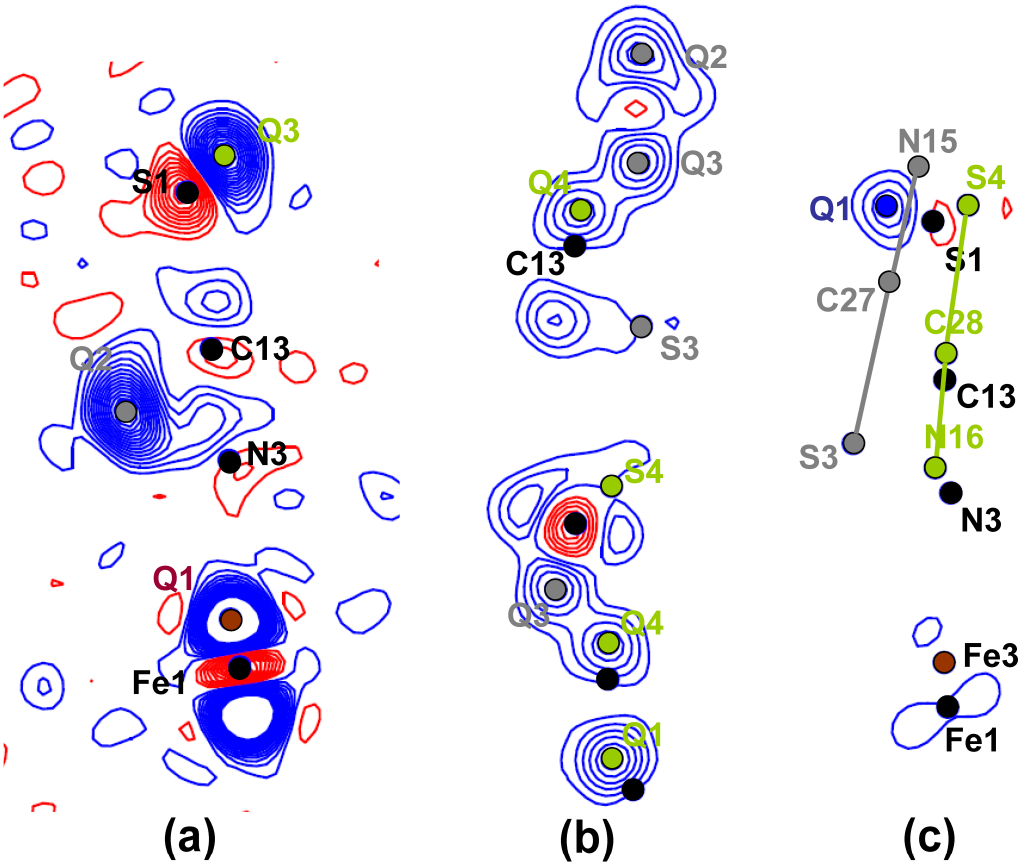

Figure S6. The difference Fourier maps based on the **MS-1** model; with negative contours in red and positive contours in blue. (a) Large negative electron density at the positions of Fe1 and N3-C13-S1 are in agreement with the existence of another major product. Three strongest residuals (Q1(brown)=50, Q2(gray)=30 and Q3(green)=25 eÅ^{-3}) can be assigned to the Fe3, S3 and S4 positions of **MS-2** from their values and positions. Contour at 2 eÅ^{-3}. (b) The C27, C28 N15 and N16 atoms on the two thiocyanates (colored in gray and green) of **MS-2** can be located from the four major residuals (Q1∼Q4 > 6 eÅ^{-3}) and linear feature. Contour at 2 eÅ^{-3}. (c) The Fe3 (green) was found to shift away (~0.4 Å) from the crystallographic inversion center and two NCS (gray and green) were located, that indicated a non-centrosymmetric **MS-2** molecule equally distributed over two orientations in the crystal. Contour at 0.5 eÅ^{-3}; the residual Q1 can then be fitted with a S4' in 20% and S4 in 80%.

(8) **Supplementary references**

S1. Sheu, C. F.; Chen, S. M.; Wang, S. C.; Lee, G. H.; Liu, Y. H.; Wang, Y. *Chem. Commun.* **2009**, 7512-7514.

S2. (a) Sheu, C. F.; Chen, K.; Chen, S. M.; Wen, Y. S.; Lee, G. H.; Chen, J. M.; Lee, J. F.; Cheng, B. M.; Sheu, H. S.; Yasuda, N.; Ozawa, Y.; Toriumi, K.; Wang, Y. *Chem.-Eur. J.* **2009**, *15*, 2384-2393; (b) Lee, J. J.; Sheu, H. S.; Lee, C. R.; Chen, J. M.; Lee, J. F.; Wang, C. C.; Huang, C. H.; Wang, Y. *J. Am. Chem. Soc.* **2000**, *122*, 5742-5747.

S3. (a) Herber, R. H. *Inorg. Chem.* **1987**, *26*, 173-178; (b) Figg, D. C.; Herber, R. H.; Potenza, J. A. *Inorg. Chem.* **1992**, *31*, 2111-2117.

S4. Shih, C. H.; Sheu, C. F.; Kato, K.; Sugimoto, K.; Kim, J.; Wang, Y.; Takata, M. *Dalton Trans.* **2010**, *39*, 9794-9800.

S5. Rigaku *RAPID-AUTO. Version 2.41 Rigaku Corporation, Tokyo, Japan.*

S6. (a) Legrand, V.; Pillet, S.; Souhassou, M.; Lugan, N.; Lecomte, C. *J. Am. Chem. Soc.* **2006**, *128*, 13921-13931; (b) Liu, H.; Su, L.; Wang, L.; Li, W. *Acta Crystallographica Section E-Structure Reports Online* **2010**, *66*, M378-U425.